Proton form factors in large N_c QCD

Teboho L. Thapedi

In partial fulfilment of the requirements
for the degree of Master of Science
at the
University of Cape Town

November 10, 2004

Abstract

The proton electromagnetic form factors are obtained using a particular model formula of QCD_∞, QCD in the large N_c limit, which sums up the infinite number of zero-width resonances to produce an Euler's Beta function, Dual-QCD_∞. The form factors $F_1(q^2)$, $F_2(q^2)$ and $G_M(q^2)$ altogether consistently agree well with reanalyzed space-like data in the whole range of momentum transfer. Additionally, the ratio $\mu_p G_E/G_M$ predictably is in good agreement with recent polarization transfer measurements at Jefferson Lab. The electric and magnetic radii are determined using this current world data.

Contents

Chapter 1

Introduction

Over a period spanning the past five decades one of the prominent efforts of strong interaction physics has been the attainment of a thorough interpretation and understanding of the internal constituent structure of the nucleons, a precursor to understanding the strong force. In a broader context, this desirability extends to a few other strongly interacting particles which consist of quarks and gluons as their fundamental basic constituents, i.e. hadrons. This has been coupled to the ambition for compatibility of theoretical and phenomenological descriptions to raw data of particular observables obtained by increasingly precision improved experimental techniques. The advent of high energy accelerators had made these data extraction undertakings aimed at revealing and testing the underlying structure of the fundamental electromagnetic and weak interactions by means of elastic, inelastic and deep inelastic scattering experiments feasible.

The present paper is a complement to the paper by Dominguez [1] comprising of work on the pion. Our focus will derive from elastic electron-proton scattering which amongst many available has proven to be a highly effective technique that could be utilized to probe and shed more light on the small distance structure of the proton. O. Stern's [2] measurement of its anomalous magnetic moment, anomalous due to discrepancy from Dirac's prediction for point-like particle ($\mu_p = \frac{e\hbar}{2M_N c}$), where e is the magnitude of the charge and M_N the nucleon mass, had provided an initial indication of possession of a complex structure. The elastic scattering process leaves the internal constituents bound and in their ground state, i.e. the proton remains on the mass shell, in a two dimensional section of momentum space possible four-momentum values lie on one sheet of a hyperboloid known as the mass shell. Illustratively, the process is: $\ell(k) + N(P) \rightarrow \ell(k') + N(P')$, where $\ell(k)$ is the lepton and its corresponding momentum and similarly for the nucleon. Of the two interaction vertices the electromagnetic interaction of the electron is understood and precisely calculable in Quantum Electro-Dynamics, by far the best known field theory, thus the electron-nucleon collision process can be interpreted in terms of the structure of the probed nucleon. The exchanged four momentum transfer which occurs in the space-like region for elastic scattering and mediating the interaction is carried by a virtual photon. The characteristic distance probed in the interaction is reciprocally related to momentum, for information more than just about the nucleon electric charge to be obtained the electron's de Broglie wavelength λ must have a magnitude comparable to the spatial extent of the nucleon. λ is supposed to be of order of, or smaller than about $1fm$. The corresponding electron's momentum must be of the order of or greater than $k = \frac{\hbar c}{\lambda} \simeq 200\, MeV$. At these energies it is highly relativistic and its energy is much larger relative to its rest mass, i.e. $E = \sqrt{\mathbf{k} + m^2} \gg m = 0.511\, MeV$.

In chapter two, for the sake of completeness, we give a broader overview of relevant concepts, definitions and pin down assumptions involved. We review the intricacies of the matrix elements of both vertices, culminating in the derivation of form factors, real Lorentz

scalar functions subsuming our ignorance of the intrinsic structure of the nucleons. Their interpretation and properties are put under scrutiny.

In chapter three we briefly outline descriptions of the methods pursued to determine data, the Rosenbluth and polarization transfer, and the extent of their reliance. Attention is also devoted to the scaling relation between the electric and magnetic form factors, elaborating on recent relevant improvements arising from the polarization transfer results.

In chapter four we cover the foundations and motivation for the Vector Meson Dominance model.

In chapter five we present QCD in the large number of colours N_c, QCD_∞, as a useful phenomenological approach as well as a detailed work out of the calculations and the results.

Chapter 2

Current matrix elements and form factors

2.1 The electron-electron vertex

We assume on the basis of the evidence of current experimental resolution that the electron is a structureless lepton, as usual spin $\frac{1}{2}$, possessing unit charge and no anomalous magnetic moment, which simplifies its interaction with the electromagnetic field. This is also important for QED because it is a local field theory describing collisions as point interactions, further, the transition matrix element is an infinite series expression, but electromagnetic interactions are dependent on a small electromagnetic coupling constant ($\alpha = \frac{e^2}{4\pi\hbar c} \cong \frac{1}{137}$) value and the perturbative approach is successful. In terms of Feynman rules an electron is represented in the initial and final states by factors $U_r(k)$ and $\overline{U_{r'}(k')}$ on the right and on the left, the fermion-photon vertex by a $ie\gamma_\mu$ factor. Accordingly, the Lorentz index is contracted with the external photon polarization vector or one of the indices of the internal photon line's propagators ($\frac{-ig_{\mu\nu}}{q^2}$). Resorting to these guidelines we express the matrix element, for an electron on mass shell, of the electromagnetic current j^{em}_μ, to which the photon couples, for momentum state k to momentum state k', of spins r and r', at the electron-photon vertex to lowest order α, i.e ignoring corrections at the vertex, by:

$$\left\langle \ell(k', r') \left| \mathbf{j}^{em}_\mu(0) \right| \ell(k, r) \right\rangle = -ie\,\overline{U_{r'}(k')}\gamma_\mu U_r(k), \tag{2.1}$$

where $\mathbf{j}^{em}_\mu(0)$ is the electron current operator evaluated at the origin in space-time, translation of the space-time point x to the origin was achieved by utilizing $\mathbf{j}^{em}_\mu(x) = e^{i(k'.x)}\mathbf{j}^{em}_\mu(0)e^{-i(k.x)}$ with the free spinor fields expressed in terms of plane waves, the $+i$ assigned to the vertex produces the correct total sign for the scattering matrix element, $U_r(k)$ and $\overline{U_{r'}(k')} \equiv U^\dagger_{r'}(k')\gamma^0$ Dirac Spinor and adjoint spinor are the positive energy eigenstates, the defined criteria met by the four vector s^μ, likewise for s'^μ, is $r.k = 0$, $r^2 = -1$ and is a polarization vector ($r^\mu = (0, \hat{\mathbf{k}})$, $\hat{\mathbf{r}}.\hat{\mathbf{r}} = 1$) in the rest frame of the electron. Only γ_μ is sandwiched between $\overline{U_{r'}(k')}$ and $U_r(k)$, so this matrix element has transformation properties of a four vector, when contracted in accordance with Feynman rules with the internal photon propagator and the nucleon vertex it yields a Lorentz invariant scattering matrix.

The electromagnetic current is a conserved quantity and this is expressed mathematically as the vanishing of the four-dimensional divergence of $j^{em}_\mu(x)$:

$$\partial^\mu j^{em}_\mu(x) = 0. \tag{2.2}$$

Consequently, this introduces a constraint on the matrix element of $j^{em}_\mu(x)$. The momentum operators $\mathbf{P}_i(i = x, y, z)$ and the energy operator P_0 (the Hamiltonian), analogous to

quantum mechanics, generate translations in space and time such that any operator obeys the commutator prescription:

$$[\mathbf{P}^{\mu}, \mathbf{F}(x)] \;=\; -i\partial_{\mu}\mathbf{F}(x) \tag{2.3}$$

We consider a matrix element of (2.2) between clearly defined arbitrary eigenstates of energy and momentum $|G\rangle$ and $|H\rangle$. Employing (2.3), we find:

$$\begin{aligned} \langle G|\,\partial^{\mu} j_{\mu}^{em}(x)\,|H\rangle &= -i\,\langle G|\,[\mathbf{P}^{\mu}, \mathbf{j}_{\mu}{}^{em}(x)]\,|H\rangle \\ &= -i\,[P_{\mu}(G) - P_{\mu}(H)]\,\langle G|\mathbf{j}_{\mu}{}^{em}(x)\,|H\rangle \;=\; 0, \end{aligned} \tag{2.4}$$

where $P_{\mu}(G)$ and $P_{\mu}(H)$ are the four momenta of these two states, if we identify $q \equiv P(G) - P(H)$ with the transferred four momentum the condition on the matrix element to vanish is:

$$q^{\mu}\,\langle G|\mathbf{j}_{\mu}{}^{em}(x)\,|H\rangle \;=\; 0. \tag{2.5}$$

By implication, for plane waves states the following condition obtains:

$$q^{\mu}\,\left\langle\, \ell(k',\, r')\,\middle|\mathbf{j}_{\mu}^{em}(0)\middle|\,\ell(k,\, r)\,\right\rangle \;=\; \overline{U_{r'}(k')}\,(\not{k}' - \not{k})\,U_{r}(k) \;=\; 0. \tag{2.6}$$

where $q^{\mu} = (k'^{\mu} - k^{\mu})$, use was made of the fact that in momentum space, the spinors $U_r(k)$ and $\overline{U_{r'}(k')}$ satisfy the Dirac equation:

$$\begin{aligned} (\not{k} - m)U_r(k) &= 0, \\ \textit{and} \qquad \overline{U_{k'}(k')}(\not{k}' - m') &= 0. \end{aligned} \tag{2.7}$$

2.2 The electron-nucleon vertex

The Feynman diagram rules for constructing matrix elements to determine an expression for the scattering matrix element are not complete for a particle with internal structure arising from interactions other than those described by QED, the particle's coupling to an external or internal photon line is not provided explicitly. The couplings could be simplified despite the shortcoming and their forms be written in terms of form factors.

The nucleon on the other hand is also a fermion, but a non-structureless bound entity of quarks and gluons and predominantly strongly interacting. The characteristic matrix element of the electromagnetic current on which restrictions emanating from current conservation, hermiticity and Lorentz covariance are imposed, assuming initial and final states on mass shell, is:

$$\left\langle\, N(P',\, s')\,\middle|\mathbf{J}_{\mu}^{EM}(x)\middle|\, N(P,\, s)\,\right\rangle \;=\; e^{i(P'-P)\cdot x}\overline{U_{s'}(P')}\Gamma_{\mu}(P,P')U_{s}(P), \tag{2.8}$$

where from Lorentz covariance $\Gamma_{\mu}(P,P')$ must satisfy:

$$S(\Lambda)\Gamma_{\mu}(P,P')S^{-1}(\Lambda) \;=\; (\Lambda^{-1})^{\mu}{}_{\nu}\Gamma^{\nu}(\Lambda P, \Lambda P'), \tag{2.9}$$

and from hermiticity:

$$\gamma^{0}\Gamma_{\mu}(P,P')^{\dagger}\gamma^{0} \;=\; \Gamma_{\mu}(P,P'), \tag{2.10}$$

where Λ is the Lorentz transformation.

Since $\mathbf{J}_{\mu}$ must transform as a Lorentz four vector in order to oblige to the covariance of the continuity equation $\partial^{\mu}\mathbf{J}_{\mu} = 0$ the assigned 4×4 matrix elements $\Gamma_{\mu}(P,P')$ which are in the spin space of the nucleon must be of choice of the most general four vector

form, the composition will obtain from P'_μ, P_μ, and the Dirac γ-matrices and their possible combinations, these are:

$$(P'+P)_\mu,\ (P'-P)_\mu,\ \gamma_\mu,\ \gamma_\mu\gamma_5,\ \gamma_5(P-P')_\mu,\ \gamma_5(P+P')_\mu,\ \sigma_{\mu\nu}(P-P')^\nu,$$
$$\sigma_{\mu\nu}(P+P')^\nu,\ \gamma_5\sigma_{\mu\nu}(P-P')^\nu,\ \gamma_5\sigma_{\mu\nu}(P+P')^\nu, \tag{2.11}$$

where

$$\gamma_5 \equiv -i\gamma_0\gamma_1\gamma_2\gamma_3 = i\gamma^0\gamma^1\gamma^2\gamma^3 \equiv \gamma^5, \tag{2.12}$$

in the standard representation, there are several different choices available, but it is not critical which one because Dirac equation's solution is specified fully by (2.16), 4×4 γ matrices are:

$$\gamma^0 \equiv \begin{pmatrix} \mathbf{1} & \mathbf{0} \\ \mathbf{0} & -\mathbf{1} \end{pmatrix},\ \gamma^k = \begin{pmatrix} \mathbf{0} & \underline{\sigma}^k \\ -\underline{\sigma}^k & \mathbf{0} \end{pmatrix},\ \gamma_5 = \begin{pmatrix} \mathbf{0} & \mathbf{1} \\ \mathbf{1} & \mathbf{0} \end{pmatrix}, \tag{2.13}$$

$\mathbf{1}$ denotes the 2×2 unit matrix and the underlined symbols Pauli matrices:

$$\underline{\sigma}^1 = \begin{pmatrix} 0 & 1 \\ 1 & 0 \end{pmatrix},\ \underline{\sigma}^2 = \begin{pmatrix} 0 & -i \\ i & 0 \end{pmatrix},\ \underline{\sigma}^3 = \begin{pmatrix} 1 & 0 \\ 0 & -1 \end{pmatrix},\ \mathbf{1} = \begin{pmatrix} 1 & 0 \\ 0 & 1 \end{pmatrix}, \tag{2.14}$$

satisfying:

$$\begin{aligned} [\sigma_i, \sigma_j] &= 2i\varepsilon_{ijk}\sigma_k \\ \varepsilon_{ijk} &= \left[\begin{array}{l} +1\ if\ (ijk)\ is\ even\ permutation\ of\ (123) \\ -1\ if\ (ijk)\ is\ odd\ permutation\ of\ (123) \\ 0\ otherwise \end{array}\right], \end{aligned} \tag{2.15}$$

the Dirac γ-matrices obey the anti-commutation property:

$$\begin{aligned} \{\gamma^\mu, \gamma^\nu\} \equiv \gamma^\mu\gamma^\nu + \gamma^\nu\gamma^\mu &= 2g^{\mu\nu} \\ in\ order\ for \qquad \gamma^\mu\gamma_\mu &= \mathbf{4I}, \end{aligned} \tag{2.16}$$

the spin tensor is:

$$\sigma^{\mu\nu} = \frac{i}{2}\left[\gamma^\mu, \gamma^\nu\right] = i\left(\gamma^\mu\gamma^\nu - g^{\mu\nu}\right), \tag{2.17}$$

the metric tensor being given by:

$$g_{\mu\nu} = \begin{pmatrix} 1 & 0 & 0 & 0 \\ 0 & -1 & 0 & 0 \\ 0 & 0 & -1 & 0 \\ 0 & 0 & 0 & -1 \end{pmatrix}, \tag{2.18}$$

$\mathbf{I}$ is the 4×4 identity matrix, the indices k run from 1 to 3, and μ and ν from 0 to 3.

The conservation of parity by electromagnetic interactions excludes all possible combinations of the above terms involving γ_5, such are pseudovectors. The remaining terms are vectors and conform to the transformation properties of the electromagnetic current operator. We obtain:

$$\begin{aligned} \left\langle N(P', s')\left|\mathbf{J}_\mu^{EM}(0)\right|N(P, s)\right\rangle = \overline{U_{s'}(P')}\big[&\gamma_\mu A_1(q^2) + i\sigma_{\mu\nu}(P'-P)^\nu A_2(q^2) \\ &+ i\sigma_{\mu\nu}(P'+P)^\nu A_3(q^2) + (P'-P)_\mu A_4(q^2) \\ &+ (P'+P)_\mu A_5(q^2)\big]U_s(P), \end{aligned} \tag{2.19}$$

Due to Lorentz invariance the form factor functions A_i's, proven to be real at the end of this section, are supposed to be Lorentz scalars and presumably dependent only on the Lorentz scalar quantities, these are P^2, P'^2, but these two are constants (i.e., $P^2 = P'^2 = M_N^2$, where M_N^2 is the nucleon mass), the only independent quantity is the product $P'P$, thus the nucleon vertex can be expressed in terms of $q^2 = (P' - P)^2$ as the only independent Lorentz invariant scalar variable. It is the square of the four momentum transfer given to the proton and for a proton initially at rest in the laboratory frame it is related to the incident and final energies as described by:

$$\begin{aligned} Q^2 \equiv -q^2 = -(k' - k)^2 = 4EE' \sin^2 \frac{\theta}{2} &= \frac{4E^2 \sin^2 \frac{\theta}{2}}{1 + \frac{2E}{M_N} \sin^2 \frac{\theta}{2}} \\ E' &= \left[\frac{E}{1 + \frac{2E}{M} \sin^2 \frac{\theta}{2}} \right], \end{aligned} \tag{2.20}$$

where θ is the in-plane scattering angle in the laboratory frame, Q^2 is as defined to avoid unnecessary minus signs, E' is the energy of the scattered and E of the incident electron.

The remaining coefficient $(P' + P)^\mu$ is expressible as a function of q^2 and the nucleon mass, for simplification of (2.19) we constitute it into form factors independent of it with these identities:

$$\overline{U_{s'}(P')}(P' + P)_\mu U_s(P) = \overline{U_{s'}(P')} \left[-i\sigma_{\mu\nu}(P' - P)^\nu + (M'_N + M_N) \right] U_s(P) \tag{2.21}$$

as well as

$$\begin{aligned} \overline{U_{s'}(P')} \left[i\sigma_{\mu\nu}(P' + P)^\nu \right] U_s(P) = \overline{U_{s'}(P')} \big[&-(P' - P)_\mu \\ &+ (M'_N - M_N)\gamma_\mu \big] U_s(P), \end{aligned} \tag{2.22}$$

which were derived from:

$$\begin{aligned} \gamma_\mu U_s(P) &= \frac{1}{M_N} (P_\mu - i\sigma_{\mu\nu}P^\nu) U_s(P) \\ \textit{and} \qquad \overline{U_{s'}(P')}\gamma_\mu &= \frac{1}{M'_N} \left(P'_\mu + i\sigma_{\mu\nu}P'^\nu \right), \end{aligned} \tag{2.23}$$

deduced from the Dirac equation (2.7), the anti-commutation property (2.16) and the spin tensor (2.17). Hence, a neat and compact outcome allowed by parity conservation and time reversal invariance is:

$$\begin{aligned} \left\langle N(P', s') \left| \mathbf{J}_\mu^{EM}(0) \right| N(P, s) \right\rangle = \overline{U_{s'}(P')} \big[&\gamma_\mu F_1(q^2) + i\frac{\kappa}{2M_N} F_2(q^2)\sigma_{\mu\nu}q^\nu \\ &+ q_\mu F_3 \big] U_s(P), \end{aligned} \tag{2.24}$$

where $\frac{\kappa}{2M_N}$ was put in by hand to comply with convention, $F_2(q^2)$'s dimension then corresponds with $F_1(q^2)$'s, and κ is the nucleon anomalous magnetic moment ($\kappa_p = 1.79$, $\kappa_n = -1.91$) in units of the nuclear magneton.

Since the limitation of current conservation and gauge invariance require compliance with the constraint (2.5), we find that:

$$\overline{U_{s'}(P')} \left[\not{q} F_1(q^2) + i\frac{\kappa}{2M_N} F_2(q^2) q^\mu \sigma_{\mu\nu} q^\nu + q^2 F_3 \right] U_s(P) = 0. \tag{2.25}$$

Employing the Dirac equation for the spinors $U_s(P)$ and $\overline{U_{s'}(P')}$, the first term is simplified to:

$$\begin{aligned} \overline{U_{s'}(P')} \not{q} F_1(q^2) U_s(P) &= \overline{U_{s'}(P')}(P' - P)^\mu \gamma_\mu U_s(P) F_1(q^2) \\ &= (M'_N - M_N) F_1(q^2) \overline{U_{s'}(P')} U_s(P) = 0, \end{aligned} \tag{2.26}$$

vanishing due to the nucleon being on mass shell, $M'_N = M_N$. The second one disappears as a result of the antisymmetric property of the spin tensor, $\sigma_{\mu\nu} = -\sigma_{\mu\nu}$. The virtual photon is off the mass shell, $q^2 \neq 0$, so $F_3 = 0$. Thus, the electromagnetic structure of the nucleon is described in terms of two independent electromagnetic form factors defined as the matrix elements of the electromagnetic current operator between nucleon states according to:

$$\langle N(P', s') \left| \mathbf{J}_\mu^{EM}(0) \right| N(P, s) \rangle = e\overline{U_{s'}(P')} \left[\gamma_\mu F_1(q^2) + i\frac{\kappa}{2M_N} F_2(q^2)\sigma_{\mu\nu}q^\nu \right] U_s(P), \quad (2.27)$$

where a factor $|e|$ was inserted at each proton vertex.

$F_1(q^2)$ and $F_2(q^2)$ are referred to as the Dirac and Pauli form factors. To ensure the correct electrostatic and magnetostatic interaction they are normalized in the limit of $q^2 \to 0$, which corresponds to the nucleons interacting with a static electromagnetic field, to: $F_1^p(0) = 1$, $F_1^n(0) = 0$ and $F_2^{p,n}(0) = 1$. Square bracket terms of equation 2.27 should require to fulfill this normalization.

We shall enquire the validity of the assumption that the form factors F_1 and F_2 are real. Utilizing the Hermiticity of the electromagnetic current yields:

$$\begin{aligned} \langle N(P, s) \left| \mathbf{J}_\mu^{\dagger EM}(0) \right| N(P', s') \rangle &= \langle N(P', s') \left| \mathbf{J}_\mu^{EM}(0) \right| N(P, s) \rangle^* \\ &= \langle N(P, s) \left| \mathbf{J}_\mu^{EM}(0) \right| N(P', s') \rangle \end{aligned} \quad (2.28)$$

Expounded, this could be related as:

$$\begin{aligned} &\left[U_{s'}(P')^\dagger \gamma_0 \left[\gamma_\mu F_1(q^2) + i\frac{\kappa}{2M_N} F_2(q^2)\sigma_{\mu\nu}(P' - P)^\nu \right] U_s(P) \right]^* \\ &= U_s(P)^\dagger \left((\gamma_0\gamma_\mu)^\dagger F_1^*(q^2) - i\frac{\kappa}{2M_N} F_2^*(q^2)(\gamma_0\sigma_{\mu\nu})^\dagger (P' - P)^\nu \right) U_{s'}(P') \\ &= \overline{U_{s'}(P')} \left[\gamma_0\gamma_\mu^\dagger\gamma_0 F_1^*(q^2) + i\frac{\kappa}{2M_N} F_2^*(q^2)\gamma_0\sigma_{\mu\nu}^\dagger\gamma_0(P - P')^\nu \right] U_s(P), \end{aligned} \quad (2.29)$$

where $\gamma_0^2 = \mathbf{I}$ was introduced between $U_s(P)^\dagger$ and the round brackets, in the second term P and P' were swopped, $\gamma_0\gamma_\mu^\dagger\gamma_0 = \gamma_\mu$ and $\gamma_0\sigma_{\mu\nu}^\dagger\gamma_0 = \sigma_{\mu\nu}$. From the equality with (2.28) it is evident that: $F_1^*(q^2) = F_1(q^2)$ and $F_2^*(q^2) = F_2(q^2)$, i.e. both form factors are real.

2.3 Interpretation and properties of form factors

2.3.1 Physical meaning

The fundamental electron-nucleon interaction consists of an electric interaction as well as a spin-spin or magnetic interaction since both particles carry spin, and the interaction vertex is analyzed in terms of the electric and magnetic form factors. The terminology of referring to F_1 as the "electric form factor" is not well grounded because it describes the electric charge and the normal Dirac magnetic moment, but F_2 is correctly associated with the anomalous magnetic moment. We are interested in how they are connected with the nucleon structure. The physical interpretation of these form factors is not unique, but dependent on a particular co-ordinate system being utilized.

The non-relativistic electron scattering form factor from a static charge distribution is expressed as a Fourier transform, but in the regime of high momentum transfers the recoil of the proton makes it impossible to analogously interpret the proton form factor. This may be overcome if we conveniently work in a particular Lorentz frame referred to as the Breit (or brick wall) frame, defined by the requirement that $P' + P$ contains no space component, i.e. the spatial three momenta of the initial and final nucleon states are equal ($\mathbf{P} = -\mathbf{P}' = \frac{\mathbf{q}}{2}$),

the electron scattering on a moving proton just reverses the momentum of the proton and its energy is left unchanged, i.e. $P_0' = P_0$, which gives $q_0 = 0$.

We evaluate the matrix element of the current operator in terms of components $\mathbf{J}_\mu^{EM}(0) \equiv (\mathbf{J}_0(0), \mathbf{J}(0))$. Making use of the Dirac equation, the following replacement may be made:

$$\begin{aligned}
\overline{U_{s'}(P')} i\sigma_{\mu\nu} q^\nu U_s(P) &= -\frac{1}{2}\overline{U_{s'}(P')}\left[\gamma_\mu, \not{P}' - \not{P}\right] U_s(P) \\
&= -\frac{1}{2}\overline{U_{s'}(P')}\left[\gamma_\mu(\not{P}' - M_N) - (M_N - \not{P}')\gamma_\mu\right] U_s(P) \\
&= \overline{U_{s'}(P')}\left[2M_N\gamma_\mu - (P' + P)_\mu\right] U_s(P), \qquad (2.30)
\end{aligned}$$

then we rewrite (2.27) in the form:

$$\langle N(P', s')\,|\mathbf{J}_\mu(0)|\,N(P, s)\rangle = e\,\overline{U_{s'}(P')}\left[\gamma_\mu\,(F_1 + \kappa F_2) - \kappa\frac{(P' + P)_\mu}{2M_N}\,F_2\right] U_s(P). \qquad (2.31)$$

The time component in the Breit frame is:

$$\begin{aligned}
\langle N(\mathbf{P}, s')\,|\mathbf{J}_0(0)|\,N(-\mathbf{P}, s)\rangle &= e\,\overline{U_{s'}(\mathbf{P})}\left[\gamma_0\,(F_1 + \kappa F_2) - \kappa\frac{E_N}{M_N}\,F_2\right] U_s(-\mathbf{P}) \\
&= 2M\delta_{s's}e\left(F_1(Q^2) + \kappa F_2(Q^2)\right) - e\kappa\frac{2E_N^2\delta_{s's}}{M_N}F_2(Q^2) \\
&= 2M\delta_{s's}e\left(F_1(Q^2) + \kappa\frac{Q^2}{4M_N^2}F_2(Q^2)\right), \qquad (2.32)
\end{aligned}$$

where $Q^2 = -4\mathbf{P}^2 = -4E_N^2 + 4M_N^2$, in the standard representation $\overline{U(\mathbf{P})}\gamma_0 U(-\mathbf{P}) = 2M_N\delta_{s's}$ and $\overline{U(\mathbf{P})}U(-\mathbf{P}) = 2E_N\delta_{s's}$ were utilized to reduce the expression.

The space components, from (2.31) the last term vanishes in the Breit frame, are given by:

$$\begin{aligned}
\left\langle N(\mathbf{P}, s')\left|\mathbf{J}^k(0)\right|N(-\mathbf{P}, s)\right\rangle &= e\,\overline{U_{s'}(\mathbf{P})}\boldsymbol{\gamma}^k U_s(-\mathbf{P})\,(F_1 + \kappa F_2) \\
&= e\,U_{s'}(\mathbf{P})^\dagger\begin{pmatrix}\mathbf{0} & \sigma^k \\ \sigma^k & \mathbf{0}\end{pmatrix} U_s(-\mathbf{P})\,(F_1 + \kappa F_2) \\
&= e\,\chi^\dagger\left[(\boldsymbol{\sigma}.\mathbf{P})\,\sigma^k - \sigma^k\,(\boldsymbol{\sigma}.\mathbf{P})\right]\chi\,(F_1 + \kappa F_2) \\
&= -2e\,\varepsilon_{kmn}P_m\chi^\dagger\sigma^n\chi\,(F_1 + \kappa F_2) \\
&= -e\,\varepsilon_{kmn}q_m\chi^\dagger\sigma^n\chi\,(F_1 + \kappa F_2) \\
&= -e\,\chi^\dagger(\mathbf{q}\times\boldsymbol{\sigma})\chi\,(F_1 + \kappa F_2), \qquad (2.33)
\end{aligned}$$

where $U_s(\mathbf{P}) = \sqrt{E + M}\begin{pmatrix}\chi_s \\ \frac{\boldsymbol{\sigma}.\mathbf{P}}{E+M}\chi_s\end{pmatrix}$.

Evidently, on the basis of (2.32) and (2.33) we can identify the electric and magnetic form factors as:

$$G_E(Q^2) \equiv F_1(Q^2) + \kappa\tau F_2(Q^2), \qquad (2.34)$$

$$G_M(Q^2) \equiv F_1(Q^2) + \kappa F_2(Q^2). \qquad (2.35)$$

The definition of these two form factors is in terms of components of the relativistically invariant four-vector current density, $\mathbf{j}(\mathbf{r})$ and $\rho(\mathbf{r})$:

$$\mathbf{j}(\mathbf{r}) = \frac{ie}{(2\pi)^3}\int d^3q\,(\boldsymbol{\sigma}\times\mathbf{q})\,G_M\,(Q^2)\,e^{i\mathbf{q}.\mathbf{r}}, \qquad (2.36)$$

$$\rho(\mathbf{r}) = \frac{e}{(2\pi)^3}\int d^3q\,G_E\,(Q^2)\,e^{i\mathbf{q}.\mathbf{r}}. \qquad (2.37)$$

So in the Breit frame the Sach's form factors, G_E and G_M, are construed as the three dimensional Fourier transforms of charge and magnetization densities of the nucleon, respectively. They were introduced by Sachs [3], and are the most convenient for quantitative analysis of data [4], opting for their use lessens the correlation of errors in the separation of form factors from data. They have been normalized in the limit $Q^2 \to 0$ to $G_E^p = 1$ (i.e. the proton's charge) and $G_M^p = \kappa_p + 1 = \mu_p$ (i.e. the proton magnetic moment). In approaching this limit the proton coupling decreases to a point-like charge as the exchanged virtual photon becomes less sensitive to the structure of the proton. The probe is with long wavelength photons, at this point the fact that the proton has structure at order of one fermi is not of significance any longer. What is observed is a particle of charge e and magnetic moment $\frac{1+\kappa_p}{2M_p}e$. For the neutron, $G_E^n = 0$ and $G_M^n = -1.91$.

2.3.2 The nucleon root mean square radii

A measure of the nucleons' finite extension, size effects i.e., to a first approximation, may be described in terms of the electric and magnetic mean square radii.

For $q << M_N$, i.e. for momentum transfers much smaller than the nucleon mass (in the nonrelativistic limit), $q_0 = E'_N - E_N \approx M'_N - M_N \approx 0$ (limit of vanishing energy), so that $q^2 = -\mathbf{q}^2$, the recoil energy of the nucleons is negligible and form factors may then be interpreted as the Fourier transform, with respect to the momentum transfer, of the charge and magnetic moment radial distributions within nucleons. Thus, we have:

$$G_E(-\mathbf{q}^2) = \frac{1}{e}\int \rho(r) e^{i\mathbf{q}.\mathbf{r}} d^3r, \tag{2.38}$$

$$\textit{and} \qquad G_M(-\mathbf{q}^2) = \int \mu(r) e^{i\mathbf{q}.\mathbf{r}} d^3r. \tag{2.39}$$

For $qr << 1$ we may expand the phase factors in (2.38) and (2.39), which account for the position dependence of the virtual photon over the size of the nucleons, in a Taylor series:

$$e^{i\mathbf{q}.\mathbf{r}} \simeq 1 + i\mathbf{q}.\mathbf{r} - \frac{1}{2}(\mathbf{q}.\mathbf{r})^2 + ..., \tag{2.40}$$

when inserted into the Fourier transforms the first terms yield the total charges, if we assume the distributions to be spherically symmetric the second terms are zero and the third are: $\frac{1}{2}\int (\mathbf{q}.\mathbf{r})^2 e_{1,2}(r) d^3r = \frac{2\pi}{3} q^2 \int e_{1,2} r^4 dr$, where e_i is either of the two distributions. So in the limit of small q:

$$\begin{aligned} G_{E,M}(-\mathbf{q}^2) &= G_{E,M}(0) - \left|\mathbf{q}^2\right| G'_{E,M}(-\mathbf{q})\,|_{\mathbf{q}^2=0} + ... \\ &= G_{E,M}(0)\left[1 - \frac{\left|\mathbf{q}^2\right|}{6}\left\langle r^2_{E,M}\right\rangle + ...\right], \end{aligned} \tag{2.41}$$

so that:

$$\begin{aligned} G_{Ep}(-\mathbf{q}^2) &\approx 1 - \frac{\left|\mathbf{q}^2\right|}{6}\left\langle r^2_{Ep}\right\rangle \\ G_{En}(-\mathbf{q}^2) &\approx -\frac{\left|\mathbf{q}^2\right|}{6}\left\langle r^2_{En}\right\rangle \\ G_{Mp,n} &\approx \mu_{p,n}\left(1 - \frac{\left|\mathbf{q}^2\right|}{6}\left\langle r^2_{Mp,n}\right\rangle\right), \end{aligned} \tag{2.42}$$

where $\left\langle r^2_E\right\rangle \equiv \frac{4\pi}{e}\int_0^\infty \rho(r) r^4 dr$, $\left\langle r^2_M\right\rangle \equiv 4\pi \int_0^\infty \mu(r) r^4 dr$, $\mu_{p,n}$ is the nucleons' magnetic moment, $\mu_p = 2.79$ and $\mu_n = -1.91$, in units of the nuclear magneton ($\frac{e\hbar}{2M_N c}$). It is obvious

from (2.41) that:

$$\langle r^2_{E,M} \rangle = 6 \frac{G'_{E,M}(-\mathbf{q}^2)\,|_{\mathbf{q}^2=0}}{G_{E,M}(0)}. \tag{2.43}$$

The r.m.s radii properties are determined form the slope of the form factor (if well behaved smooth functions of $\mathbf{q}^2$) at $\mathbf{q}^2 = 0$, however, extrapolation to $\mathbf{q}^2 = 0$ of the form factor curve in practice is necessary to account for the appreciable gap between momentum transfer experimentally possible and $\mathbf{q}^2 = 0$.

Since for sufficiently small $\mathbf{q}^2$ the contributions of the higher order terms in the series expansion (2.41) are negligible, $G_{E,M} = \delta_{E,M} + \beta_{E,M}\mathbf{q}^2$ or an appropriate truncation put to the test may be fit to low momentum cross section form factors (discussed in chapter 3) in a wide interval near $\mathbf{q}^2 = 0$ and then the parameters determined from the best fit. The r.m.s radii obtained form this fit are model independent. Under form factor scaling assumption (elaborated about in chapter 3) reliable results are obtained still because there is no evidence of its significant deviation at very low momentum transfer.

Chapter 3

Measurement techniques and scaling

3.1 The Rosenbluth route

Data acquisition on form factors from which integral information of our qualitative and quantitative analysis will consist is obtained from cross-section measurements, such are expressed to the lowest order in the electromagnetic coupling constant α, i.e. in the one photon exchange approximation, by the Rosenbluth technique [5]. This assumed one photon exchange dominance in the elastic electron-proton collision process was established by the earliest work of Chambers and Hofstadter [6]. The prescribed differential cross section formula, which is used after radiative corrections have been applied, in the limit that the electron mass can be neglected compared with energy is expressed in the form:

$$\frac{d\sigma}{d\Omega} = \sigma_{NS}\left[F_1^2(Q^2) + \tau\kappa_p^2 F_2^2(Q^2) + 2\tau\left[F_1(Q^2) + \kappa_p F_2(Q^2)\right]^2 \tan^2\frac{\theta}{2}\right], \tag{3.1}$$

where $\tau = \frac{Q^2}{4M_p^2}$, form factors $F_1(Q^2)$ and $F_2(Q^2)$ describe the helicity-conserving and helicity flip scattering amplitudes, σ_{NS} is the non-structure cross-section, i.e. scattering from a point no structure proton and is of form:

$$\begin{aligned}\sigma_{NS} \equiv \left(\frac{d\sigma}{d\Omega}\right)_{NS} &= \frac{(\alpha\hbar c)^2\cos^2\frac{\theta}{2}}{4E^2\sin^4\frac{\theta}{2}}\frac{1}{1+2\frac{E}{M_p}\sin^2\frac{\theta}{2}} \\ &= \left(\frac{d\sigma}{d\Omega}\right)_{Mott}\frac{E'}{E},\end{aligned} \tag{3.2}$$

$\left(\frac{d\sigma}{d\Omega}\right)_{Mott}$ is the cross-section for scattering of electrons by a coulomb field, i.e. a spin-less point charge with mass of proton.

This technique is sensitive to systematic errors in E', E and θ due to being entirely dependent on cross section measurements.

The appearance of cross terms F_1F_2 in the Rosenbluth formula complicates the analysis of data, but a simplification can be achieved by rewriting it in terms of the Sach's electric and magnetic form factors, G_E and G_M. They are introduced, in accordance with how they are defined in section 2.3, then interference terms of the form G_EG_M do not occur in the cross section, thus avoiding mixing effects of the charge and magnetization distributions. We end up with a linear combination of the squared form factors in the cross section. So

the differential cross section is rewritten:

$$\frac{d\sigma}{d\Omega} = \sigma_{NS}\left[\frac{G_E^2(Q^2) + \tau G_M^2(Q^2)}{1+\tau} + 2\tau G_M^2(Q^2)\tan^2\frac{\theta}{2}\right]. \tag{3.3}$$

Extraction of form factors is facilitated by converting the differential cross section into a form that permits independent separation of form factors:

$$\sigma_R \equiv \frac{d\sigma}{d\Omega}\frac{(1+\tau)}{\sigma_{NS}}\epsilon = \epsilon G_E^p(Q^2) + \tau G_M^p(Q^2), \tag{3.4}$$

where σ_R is the reduced cross section and ϵ is the virtual photon longitudinal polarization, for specific Q^2 values it is only dependent on the scattering angle:

$$\begin{aligned} \epsilon &= \left[1 + 2(1+\tau)\tan^2\frac{\theta}{2}\right]^{-1}, \\ 0 &\leq \epsilon \leq 1. \end{aligned} \tag{3.5}$$

The Slope (G_E) and intercept (τG_M) are determined from a good characterization of data obtained from performing a linear best fit to the reduced cross section evaluated at fixed momenta but varying ϵ. The rectilinear relation (3.4) is characteristic of single photon exchange and has been observed to hold experimentally to a good accuracy, thus providing indication of no significant deviations from the Born approximation. The validity of this assumption is also confirmed by the consistency of (3.3) in successfully describing positron scattering as well. On the other hand, application of higher order radiative corrections to experimental data, effectively including more than one photon exchange, could effect an impact on the reduced cross section versus ϵ slope, subsequently having an appreciable effect on the form factors ratio value. Double exchange may occur, however, the fact that the cross sections for e^+P and e^-P are equal, as opposed to the expectant result to the contrary, is indicative of its insignificance. The Rosenbluth plots provides for a demonstrable statistical correlation to be observed between G_E and G_M. The obtained values are independent of the mathematical expression (3.4) being true in nature.

The utility of the Rosenbluth procedure to extract form factors is severely limited at large Q^2 values, for $Q^2 > 1$ the harder the measurement of G_E due to its minor contribution to the differential cross section and amongst different experimental groups there exist large comparative uncertainties and inconsistencies. The τ factor which is directly proportional to Q^2 gives rise to incremental dominance of G_M over G_E. The electric force conforms to a squared reciprocal dependence ($\sim \frac{1}{r^2}$), but the magnetic force is related by cubic form ($\sim \frac{1}{r^3}$), consequently at shorter distances the latter assumes a larger role. At large Q^2 fractional uncertainties in G_E^2 are amplified into bigger proportions compared to those on cross sections due to their minor contribution, but G_M^2's uncertainties remain relatively small up to a Q^2 value of 31.2 GeV^2. Large four-momentum transfer squared measurements are crucial for putting the perturbative QCD scaling predictions for the helicity conserving and helicity non-conserving terms, F_1 and F_2 to the test.

Energy and momentum conservation at the nucleon vertex yields the condition:

$$P + q = P'. \tag{3.6}$$

Since elastic scattering provides for the nucleon to remain intact subsequent to exchange of a virtual photon, we find:

$$P.q = -q^2. \tag{3.7}$$

Consequently, a condition obeyed by elastic scattering is:

$$\nu \equiv \frac{Q^2}{2M_N}, \tag{3.8}$$

where $\nu = E - E'$ is the energy lost to the nucleon.

3.2 The polarization transfer method

The Rosenbluth plots have traditionally been utilized in the past to determine the separation of the electromagnetic nucleon form factors. A different, highly precise and efficacious technique is the polarization transfer technique, it measures the ratio of the form factors. In the one photon exchange approximation longitudinally polarized electrons scatter off and transfer polarization to the recoil proton with only two non zero helicity dependent polarization components, P_t and P_ℓ, which are in the electron scattering plane, the former transverse to and the latter longitudinal to the proton's momentum. Accordingly:

$$P_t = \frac{h}{I_0}\left(-2\sqrt{\tau\,(1+\tau)}\,G_M^P G_E^P \tan\frac{\theta_e}{2}\right), \tag{3.9}$$

$$P_\ell = \frac{h\,(E_e + E_e')}{I_0 M_p}\sqrt{\tau\,(1+\tau)}\,\left(G_M^P\right)^2 \tan^2\frac{\theta_e}{2}, \tag{3.10}$$

where h is the electron beam helicity, $I_0 = G_E^2 + \frac{\tau}{\epsilon}G_M^2$. The ratio of the form factors can be obtained by a combination of (3.9) and (3.10):

$$\frac{G_E^p}{G_M^p} = -\frac{P_t}{P_\ell}\frac{(E+E')\tan\frac{\theta_e}{2}}{2M_p} \tag{3.11}$$

The ratio of the two form factors is easier to measure and is determined from a simultaneous measurement of the two recoil polarization observables, thus circumventing the influential systematic uncertainty obstacle confronting the Rosenbluth technique. The knowledge of spin transport is the only prominent systematic uncertainty, though magnitude relatively and significantly small compared to those in cross section measurements.

This method offers a significantly improved ratio outcome at high values of Q^2, but lack of consistency compared to the Rosenbluth method exists within the same boundary of measurements [7]. This absence of consistency diminishes the absolute certainty with which G_E^p can be known and to a comparatively less extent G_M^p as well. It cast doubt on the viability and correctness of making use of the proton form factors in different measurements which include the electromagnetic interaction of the proton, and as well as on the certainty of theoretical models prescribed to by data.

A better and precise measurement of form factors is desirable and essential. At increasingly high transfer of momentum they provide crucial details on the quark structure within nucleons, and more importantly information on the nature of the strong force at moderate inter-quark separation, thus providing a fundamental understanding of the strong force. Their precise determination provides constraints on models of baryon structure, more especially limits on the validity of any QCD based theory. The experimental results of reactions of electrons scattering from nucleons or nuclei including electromagnetic interactions make use of form factors as one of the vital phenomenological properties and as an aid tool for calculations.

The discrepancy between the Rosenbluth and Polarization measurements is interpreted as a two-photon exchange correction which impacts the former more than the latter. Once performed (i.e. the two photon correction), both techniques agree with each other [7].

3.3 Form factor scaling

The first of its kind experimental undertaking by Hofstadter and his collaborators at Stanford, in 1961, brought to bear evidence of deviation of scattering from that expected for a point particle proton. This was also accompanied by an empirical discovery that their

results could be satisfactorily summarized by a simple scaling law:

$$G_E^p(Q^2) \approx \frac{G_M^p(Q^2)}{\mu_p} \approx G_D(Q^2) = \left(1 + \frac{Q^2}{0.71}\right)^{-2}, \tag{3.12}$$

where Q^2 is in GeV^2. This implies that the magnetic moment and charge distributions conform to the same spatial dependence. This law is by definition true in the limit of $Q^2 \to 0$, and is also equal to $\frac{G_M^n(Q^2)}{\mu_n}$. The parametrization G_D is the form factors' dipole approximation, a lowest order endeavor taking account of the finite extension of the nucleon. It corresponds to an exponential rather than a Yukawa type (its significance is not understood) charge-magnetic moment spatial distribution. So it may be interpreted as:

$$\rho(r) = \rho_0\, e^{-\frac{r}{r_0}}, \tag{3.13}$$

where r_0 is defined as the scale of the nucleon radius.

The dipole formula was invented for low four-momentum transfer squared values and the obtained fit is relatively successful. At high momentum transfer the quasi on-shell constituent quarks' electromagnetic structure intervenes in determining the entire nucleon form factor momentum transfer dependence. The aftermath of which is that the dipole formula extrapolation to these large values is dogged by noticeably large corrections.

Recent data [8, 9, 10] of the ratio $\frac{G_E^p}{G_M^p}$ from the polarization transfer measurements confirmed deviation from factor scaling ($\frac{\mu_p G_E^p}{G_M^p} \approx 1$), contrary to expectation. The observations indicated that the ratio actually decreases as Q^2 is increased. A demonstration that the electric and magnetic distributions are in effect dissimilar.

For reasons outlined in chapter three the Rosenbluth method form factor scaling results on their own are not dependable. So in chapter 5 calculations will be performed using data assessed on the basis of this latest modification as a constraint.

Chapter 4

Vector Meson Dominance models

Several efforts have been expended to allocate the best fit to the four momentum transfer dependence of the nucleon form factors with a variety of functional forms inspired from theoretical models of hadronic structure. The extent of statistical consistency and qualitative agreement with data in regions of low, moderate and high Q^2 has been of varying degrees of success, and not necessarily comparable in all regions.

Vector Meson Dominance models [11] describe the electromagnetic interaction process by employing an assumption that the virtual photon couples to the proton via an intermediate vector meson (see figure). These are strongly interacting particles possessing the quantum numbers of the photon: zero charge, zero strangeness and $J^{PC} = 1^{--}$. The first prerequisite is met by obliging the vector meson to be an isotopic spin zero object or the neutral member of an isospin multiplet. These resonances whose existence was predicted even prior to their discovery are the ρ, ω and ϕ. The prediction of the first two from nucleon form factors laid the groundwork. Nambu (1957) proposed the existence of the ω. This was to account for conflict between experimental observation $F_1^n \sim 0$ and the then theory ($eF_1^p = -eF_1^n$). Charged clouds were considered composed entirely of uncorrelated pions so that ($P \leftrightarrow n+\pi^+$ and $n \leftrightarrow P+\pi^-$). The photon then experiences $e_{\pi^+} = -e_{\pi^-}$. Frazer and Fulco's suggestion of the existence of the ρ, in 1961, was geared at explaining the isovector hadronic form factor $F_1(q^2)$.

Various models developed within this framework differ by the quantity of vector meson intake in calculations, others utilize the bare photon coupling, some the meson width. Couplings, vector mesons' masses and number of mesons have been varied to fit data. However, the models are of practical use only if there is a limit to the quantity of these adjustable parameters. A thorough insight into the binding dynamics of confined quarks within hadrons is a fundamental prerequisite for carrying out electromagnetic form factor calculations without utilizing parameters. However, there exist no analytical solutions to the theory of strong interactions (i.e. Quantum Chromodynamics) at low-intermediate momentum transfers. A common feature of all models is that they incorporate the ρ and ω mesons, which are of the lowest mass, but use of higher mass mesons of type such as ϕ, ω', ρ' and ρ'' is not shared by all models. All formulations of vector dominance are not fundamental, i.e. they fall far short of being complete. Their applicability is mostly constrained to low/moderate Q^2. They have not had success at predicting the masses or the quantity of mesons. If in conjunction with conserved vector current it were exact then the ρ, ω and ϕ, analogous to the universal coupling of the photon to all charged particles, it would couple to all hadron states in a universal fashion. The idea of the conserved vector current is to treat j_μ^s and $j_\mu^{v,i}$, the isoscalar and isovector components, as conserved hadronic currents.

The contribution of the vector mesons to the nucleon form factors is expressed as a sum over meson propagators (partially contributing to Q^2 dependence of form factors) times vector meson-nucleon and vector meson-virtual photon coupling terms. The four independent isovector ($I = 1$ for $V = \rho$,...) and isoscalar ($I = 0$ for $V = \omega$, ϕ,...) form factors are:

$$F_{1,2}^{V,S}(Q^2) = \sum_V \frac{M_V^2}{M_V^2 + Q^2} \frac{g_{1,2VNN}}{\gamma_V}, \tag{4.1}$$

where:
(i) g_{1VNN} is the vector meson-nucleon coupling term if helicity is conserved and g_{2VNN} the vector meson-nucleon coupling term if helicity is transferred. They are assumed to have no additional Q^2 dependence.
(ii) M_V is the mass of a meson resonance.
(iii) Single poles $\frac{1}{M_V^2+Q^2}$ are the meson propagators (finite width of vector mesons have been neglected).
(iv) γ_V are the virtual photon-vector meson coupling terms. They are determined from the widths of the leptonic decays:

$$\frac{\gamma_V^2}{4\pi} = \frac{\alpha^2}{3} \frac{M_V}{\Gamma(V \to e^+e^-)}. \tag{4.2}$$

The isovector form factor component reverses sign under isospin rotation, while the isoscalar stays invariant, only interchanging a proton and a neutron. They are not normalized independently, for specific isospin states:

$$\begin{aligned} F_{1,2}^p &= \frac{1}{2}\left(F_{1,2}^V + F_{1,2}^S\right), \\ F_{1,2}^n &= \frac{1}{2}\left(F_{1,2}^V + F_{1,2}^S\right), \\ F_{1,2}^V &= \left(F_{1,2}^p - F_{1,2}^n\right), \\ F_{1,2}^S &= \left(F_{1,2}^p + F_{1,2}^n\right). \end{aligned} \tag{4.3}$$

Equation 4.1 may be obtained as a special case of a general dispersion theory used to tackle nucleon form factors. Dispersion relations have been employed as a basis for a physical understanding of the form factors. The approach taken was to assume form factors as analytic functions in the whole $-q^2$ plane, except over a branch cut from the threshold Q_0^2 to ∞. In the space like region form factors have been assigned to integrals over the imaginary part of the form factor, i.e. the spectral function, in the time-like region. Under the assumed analyticity and with no subtractions needed the following dispersion relation is valid:

$$F_{1,2}(Q^2) = \frac{1}{\pi} \int_{Q_0^2}^{-\infty} \frac{Im\, F(Q'^2)}{Q'^2 - Q^2}\, dQ'^2, \tag{4.4}$$

where Q_0^2 is $4m_\pi^2$ for the isovector and $9m_\pi^2$ for the isoscalar states. This reproduces equation 4.1 if $Im\, F(Q'^2)$ is replaced by $Im\, F(Q'^2) = A_{1,2}\pi\delta\left(Q'^2 - M_V^2\right)$. We take $A_{1,2} = \frac{M_V^2}{\gamma_V^2} g_{1,2VNN}$.

The defining characteristic feature of the isovector form factors in VMD is single-ρ-dominance. Be as it may, its validity has to be probed with experimental data. We wish to investigate two particular cases, the pion and the proton. The former is given by:

$$F_\pi(Q^2) = \frac{M_\rho^2}{M_\rho^2 + Q^2} \frac{g_{\rho\pi\pi}}{\gamma_\rho}. \tag{4.5}$$

In accordance with the normalization $F_\pi(0) = 1$:

$$\frac{g_{\rho\pi\pi}}{\gamma_\rho} = 1, \tag{4.6}$$

obtaining universality, but experimentally:

$$\frac{g_{\rho\pi\pi}}{\gamma_\rho} = 1.21 \pm 0.02. \tag{4.7}$$

The violation of universality may be interpreted as firm evidence for the existence of radial excitations of the ρ-meson. This discrepancy with experimental data is satisfactorily addressed as described in chapter five.

On the other hand the proton form factors (normalized to $F_{1,2}(0) = 1$) are given by:

$$F_{1,2}(Q^2) = \frac{M_\rho^2}{M_\rho^2 + Q^2} \frac{g_{1,2\rho NN}}{\gamma_\rho}. \tag{4.8}$$

From which:

$$\frac{g_{1,2\rho NN}}{\gamma_\rho} = 1. \tag{4.9}$$

Deviations from this universality relation are expected due to contributions from the radial excitations. In addition, according to quark counting rules in perturbative QCD, $F_2(Q^2)$ is expected to fall off faster than $F_1(Q^2)$ for large Q^2. Hence, the correction to Eq. (4.9) for $g_{2\rho NN}$ should be larger.

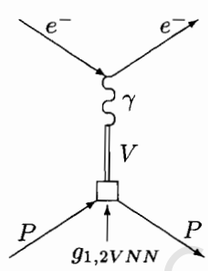

Fig. 5.1: A display of VMD

Chapter 5

Proton form factors in large N_c QCD

5.1 Phenomenological exploits of QCD_∞

Quantum chromodynamics in the limit of a large number of colours, QCD_∞ [12], is established to predict a hadronic world comprising of an infinite number of zero-width resonances [13]. The reality, however, is that QCD is dogged by the absence of exact and analytical solutions, as such fundamental hadronic parameters appearing in its Lagrangian are still to be determined. This is a fundamental challenge on its own by which the validity of QCD as a field theory of hadronic strong interactions is to be measured. Since it has not been possible to predict these undetermined parameters (quark masses m_f, where f denotes different quark flavours, and the strong coupling constant) they are extracted from experiment. In reference to the hadronic spectrum as above, a number of models have been proposed for heavy quark Green's functions [14-15] as well as for light quark systems [16]. The infinite number of zero width resonances of QCD in the limit of a large number of colours is reminiscent of Veneziano's dual resonance model [17]. Taking lead from this model has led to a development referred to as Dual-QCD_∞ [1], a particular realization of QCD_∞ in which the masses and couplings in a Green's function are picked out to produce an Euler's Beta function of the Veneziano type. In this framework the form factors (for three point functions) possess asymptotic Regge-behaviour (power behaviour) in the space-like region which is determined by a single parameter. Successful application of Dual-QCD_∞ for the pion electromagnetic form factor in the space-like region is exploited in [1]. Results contained therein provide a highly consistent agreement with experiment surpassing for example naive Vector Meson Dominance or even perturbative QCD [18]. This level of agreement also holds for the pion mean-square radius as well as for the deviation from universality of the ratio $g_{\rho\pi\pi}/f_\rho$. Additionally, prediction of the vector two-point spectral function in the time like region is arrived at from unitarization of Dual-QCD_∞, agreeing reasonably well with data. In reference [19] a more refined model in the time like region has been recently proposed. On account of the utilities and successes of the Dual-QCD_∞ model, our analysis will be inspired with its framework.

During the earliest three point functions (involving in excess of one form factor [20]) dual resonance model applications it was not clearly distinct which form factor or a linear combination of them the model should be applicable to. Dual-QCD_∞ is free of any ambiguities, mainly attributable to this formalism being manifested within the confines of a quantum field theory. The form factors should necessarily feature in the primary hadronic spectral function, dual to the spectral function of the QCD field theory. These are bound to be

the form factors characteristic of the correct pole structure required by dispersion relations in the complex energy plane. For the nucleon, these are namely the Dirac and Pauli form factors, in QCD_∞ they take the form:

$$F_{1,2}(s) = \sum_{n=0}^{\infty} \frac{C_{(1,2)n}}{(M_n^2 - s)} , \tag{5.1}$$

where $s \equiv q^2$, the masses of the vector-meson zero-width resonances M_n and their couplings C_{1n} as well as C_{2n} remain unpredicted. In the chosen formalism they are picked on to ensure that the form factors are Beta functions, ratios of gamma functions:

$$C_{(1,2)n} = \frac{\Gamma(\beta_{1,2} - 1/2)}{\alpha'\sqrt{\pi}} \frac{(-1)^n}{\Gamma(n+1)} \frac{1}{\Gamma(\beta_{1,2} - 1 - n)} , \tag{5.2}$$

where $\beta_{1,2}$ are free parameters governing the asymptotic behaviour in the space-like region ($s < 0$), and $\alpha' = 1/2M_\rho^2$ is the universal string tension in the rho-meson trajectory:

$$\alpha_\rho(s) = 1 + \alpha' \left(s - M_\rho^2\right) . \tag{5.3}$$

The chosen mass spectrum (as in [21]) is:

$$M_n^2 = M_\rho^2 (1 + 2n) . \tag{5.4}$$

Replacing (5.2) and (5.4) in (5.1) yields:

$$\begin{aligned} F_{1,2}(s) &= \frac{\Gamma(\beta_{1,2} - 1/2)}{\sqrt{\pi}} \sum_{n=0}^{\infty} \frac{(-1)^n}{\Gamma(n+1)} \frac{1}{\Gamma(\beta_{1,2} - 1 - n)} \frac{1}{[n + 1 - \alpha_\rho(s)]} \\ &= \frac{1}{\sqrt{\pi}} \frac{\Gamma(\beta_{1,2} - 1/2)}{\Gamma(\beta_{1,2} - 1)} B(\beta_{1,2} - 1,\ 1/2 - \alpha' s) , \end{aligned} \tag{5.5}$$

where $B(x, y)$ is Euler's Beta function. In the time-like region ($s > 0$) the Beta function poles are identified with an infinite set of zero-width resonances with equally spaced squared masses provided by (5.3). Take note that (5.5) reproduces:

$$Im F_{1,2}(s) = \frac{\Gamma(\beta_{1,2} - 1/2)}{\alpha'\sqrt{\pi}} \sum_{n=0}^{\infty} \frac{(-1)^n}{\Gamma(n+1)} \frac{1}{\Gamma(\beta_{1,2} - 1 - n)} \pi\, \delta\left(M_n^2 - s\right) . \tag{5.6}$$

Finite-width corrections are crucial in the time-like region. Starting from infinitely narrow resonances in the space-like region where form factors have been measured, these corrections are achieved by means of a unitarization scheme. An extrapolation to the time-like region via this prescription is not ideal or useful, for the nucleon, because the threshold for the photon to convert to nucleons is $4M_N^2$ and this is far removed from the origin. The same argument, however, for the pion is not valid because $4M_\pi^2$ is not as far removed from the origin.

In the space-like region the form factors, asymptotically, obey Regge-behaviour:

$$\lim_{s \to -\infty} F_{1,2}(s) = (-\alpha' s)^{(1 - \beta_{1,2})} , \tag{5.7}$$

The free parameters $\beta_{1,2}$ are determined from data in the space-like region. Take cognizance that for $\beta_{1,2} = 2$ the form factors are simplified to single rho-meson dominance, i.e. naive Vector Meson Dominance. According to (5.4), the mass formula, the first three predicted radial excitations are: $M_{\rho'} \simeq 1340$ MeV, $M_{\rho''} \simeq 1720$ MeV, and $M_{\rho'''} \simeq 2034$ MeV agreeing reasonably with experiment [22]: $M_{\rho'} = 1465 \pm 25$ MeV, $M_{\rho''} = 1700 \pm 20$ MeV, and

$M_{\rho'''} = 2149 \pm 17$ MeV. If we were to match the asymptotic Regge behaviour to the Operator Product Expansion of current correlators at short distances alternative, nonlinear, mass formulas might be necessary [23]. The differences in the values of the first few masses, despite this consideration, are at the expectation of a few percent. It follows then that the effect on the form factors would not be considerate due to the factorial suppression of contributions from high mass states.

5.2 Calculations

Measurements of elastic electron-proton scattering cross sections, the Rosenbluth method [24] also outlined in chapter 3, have traditionally been pursued to determine Sachs form factors. The empirical approximate scaling relation (elaborated about in chapter 3 as well) $\mu_p G_E(q^2)/G_M(q^2)$ had been shown to hold up to $-q^2 \equiv Q^2 \simeq 7$ GeV when direct extractions of $G_E(q^2)$ and $G_M(q^2)$ were exercised. In accordance with explanations contained in chapter 3 $G_E(q^2)$'s determination present difficulties. Apart from this, at Jefferson Lab (Jlab) [8, 10, 25] recent electron-proton polarization transfer measurements up to $Q^2 \simeq 6$ GeV had indicated non-negligible deviation from the scaling relation, with the exception of very small Q^2 [26]. A close scrutiny of the discrepancies between the two measurements routes is offered in [27], indications are that the source of this discrepancy is given rise to by the two-photon exchange contributions [28]. This forms the basis of our assumption and our data is limited by corrections as highlighted in [29]. The objective of these corrections is to bring in agreement with regard to $\mu_p G_E(q^2)/G_M(q^2)$. Within this prescription $F_1(q^2)$ and $F_2(q^2)$ data points are obtained with the aid of (2.34) and (2.35). We find $\beta_1 = 3.03$ and $\beta_2 = 4.20$ after fixing fits to this data. Results for $F_1(q^2)$ and $F_2(q^2)$ (with the best $\beta_{1,2}$) fits are shown in figures 1 and 2, together with the raw data [29]. $G_M(q^2)$'s results are shown in fig. 3 using (2.35) and the fitted $F_{1,2}(q^2)$. The level of agreement between (5.5) and the data is satisfactorily very good. We anticipate our theoretical form factors to yield a ratio $\mu_p G_E(q^2)/G_M(q^2)$ in obedience with experiment since our fitted data is corrected on account of the polarization transfer data on this ratio. This holds up, but with a powerful correlation between $\beta_1 - \beta_2$, this ratio is highly sensitive to a pair of these. The theoretical prediction of the ratio which corresponds to $\beta_1 = 3.0$ and $\beta_2 = 4.2$ accompanied by the JLab data is shown in fig. 4. Correlated pairs producing equally good fits result from a slight variation of these parameters, illustratively a near identical theoretical prediction is obtained with the pair $\beta_1 = 2.95$ and $\beta_2 = 4.13$. A performance of a combined fit to $F_1(q^2)$, $F_2(q^2)$ and the ratio $\mu_p G_E(q^2)/G_M(q^2)$ ends up with:

$$\begin{aligned} \beta_1 &= 2.95 - 3.03 \\ \beta_2 &= 4.13 - 4.20. \end{aligned} \tag{5.8}$$

The mean-squared electromagnetic radii resulting from (5.5) are:

$$\langle r^2_{1,2} \rangle = 6\,\alpha' \left[\psi\left(\beta_{1,2} - 1/2\right) - \psi\left(1/2\right) \right], \tag{5.9}$$

where $\psi(x)$ is the digamma function. Utilizing the ingredients from (5.8) in (5.9) yields $\langle r_1^2 \rangle^{1/2} = 0.72$ *fm* and $\langle r_2^2 \rangle^{1/2} = 0.78$ *fm*. Adopting (2.34) and (2.35) these radii reproduces the Sachs radii $\langle r_E^2 \rangle^{1/2} = 0.81$ *fm*, and $\langle r_1^2 \rangle^{1/2} = 0.76$ *fm*. These values are reasonably comparable with those that occur in the literature [30], due regard should be given to the fact that the free parameters have been determined from the whole large Q^2 data range $0 \leq Q^2 \lesssim 30$, and in the same range the form factors decrease by three to four orders of magnitude. Attention should also be paid to the fact that the extractions might be impacted upon by the strong deviation from unity of the ratio $\mu_p G_E(q^2)/G_M(q^2)$.

If we do take as an approximation that $\beta_2 \simeq \beta_1 + 1$ and make use of the properties of the gamma function the ratio is obtained to take the form:

$$r \equiv \frac{\mu_p G_E(q^2)}{G_M(q^2)} = \mu_p \frac{\left(\beta_1 - \frac{1}{2}\right) + Q^2\left[\alpha' - \frac{\kappa_p}{4M_p^2}\left(\beta_1 - \frac{1}{2}\right)\right]}{\mu_p\left(\beta_1 - \frac{1}{2}\right) + \alpha' Q^2}. \tag{5.10}$$

The predicted $r = 0$ for $\beta_1 = 2.95$ and 3.03 occurs at the corresponding values of 8.0 and 7.4 GeV^2 respectively. In general, however, $r = 0$ at:

$$F_1(\beta_1, Q^{*2}) = \frac{\kappa_p Q^{*2}}{4M_p^2} F_2(\beta_2, Q^{*2}) \tag{5.11}$$

A computer programme written to seek the zeros, where $F_{1,2}(\beta_{1,2}, Q^2)$ are derived from (5.5), confirms that they do indeed exist in apparent agreement with the logic of the approximation made that $\beta_2 \simeq \beta_1 + 1$. The existence of a zero for the ratio r is an interesting prediction of the model. New data from Jefferson Lab should be a valuable test of this result.

Chapter 6

Conclusion

The comparison of dual-QCD_∞'s nucleon form factors $F_1(q^2)$ and $F_2(q^2)$ is in quantitative agreement with the space-like region corrected experimental data [28] (for $0 \leq Q^2 \leq 30GeV^2$). The agreement of the model with the correct behaviour of G_M, the Sachs magnetic form factor, is extremely good. The prediction for the specially important ratio $\mu_p G_E(q^2)/G_M(q^2)$ is as good. From a theoretical point of view the overall picture that emerges from the above results is that dual-QCD_∞ is a satisfactorily model capable of describing the essential features of QCD in the large N_c limit.

Acknowledgement

It is a pleasure to express my gratitude and appreciation to Prof. C.A. Dominguez, my supervisor, for his interest, valuable insight, guidance and assistance throughout the thesis.

I would like to thank the National Research Fund for financial assistance for the past duration of two years.

Bibliography

[1] C.A. Dominguez, Phys. Lett. B 512 (2001) 331.

[2] O. Stern, Nature 132 (1933) 103.

[3] R.G. Sachs, Phys. Rev. 126 (1962) 2256.

[4] L.N. Hand, D. Miller and R. Wilson, Rev. Mod. Phys. 35 (1963) 335; K.J. Barnes, Phys. Lett. 1 (1962) 66.

[5] M.N. Rosenbluth, Phys. Rev. 79 (1950) 615.

[6] E.E. Chambers and R. Hofstadter, Phys. Rev. 103 (1956) 1454.

[7] J. Arrington, nucl-ex/0305009 (2003).

[8] M.K. Jones *et al.*, Phys. Rev. Lett. 84 (2000) 1398.

[9] O. Gayou *et al.*, Phys. Rev. C 64 (2001) 038292.

[10] O. Gayou *et al.*, Phys. Rev. Lett. 88, (2002) 092301.

[11] J.J. Sakurai, *Currents and Mesons*, University of Chicago Press (1969).

[12] G. 't Hooft, Nucl. Phys. B 72 (1974) 461.

[13] E. Witten, Nucl. Phys. B 79 (1979) 57.

[14] B. Chibisov et al. J. Mod. Phys. A 12 (1997) 2075; B. Blok, M. Shifman and Da-Xin Zhang, Phys. Rev. D 57 (1998) 2691.

[15] P. Colangelo, C.A. Dominguez and G. Nardulli, Phys. Lett. B 409 (1997) 417.

[16] S. Peris, B. Phily, E. de Rafael, Phys. Lett. 86 (2001) 14, and references therein.

[17] P.H. Frampton, *Dual Resonance Models*, Benjamin (1974).

[18] C.A. Dominguez, Phys. Rev. D 25 (1982) 3084.

[19] C. Bruch, A. Khodjamirian, J.H. Kühn, hep-ph/0409080 (2004).

[20] P.H. Frampton, Phys. Rev. D 1 (1970) 3141; R. Iengo, E. Remiddi, Nuovo Cimento Lett. 18 (1969) 922; C.A. Dominguez, O. Zadron, Nucl. Phys. B 33 (1971) 303; C.A. Dominguez, Phys. Rev. D 8 (1973) 980.

[21] This mass formula was first proposed in a different context by A. Bramon, E. Etim, M. Greco, Phys. Lett. 41 B (1972) 609; M. Greco, Nucl. Phys. B 63 (1973) 398.

[22] Particle Data group, K. Hagiwara *et al.*, Phys. Rev. D 66 (2002) 010001.

[23] S.S. Afonin, A.A. Andrianov, V.A. Andrianov, D. Espriu, J. High Energy Phys. 04 (2004) 039.

[24] T. Janssens *et al.*, Phys. Rev. D 142 (1966) 922; J. Litt *et al.*, Phys. Lett. 31 B (1970) 40; Ch. Berger *et al.*, Phys. Lett. 35 B (1971) 87; W. Bartel *et al.*, Nucl. Phys. B 58 (1973) 429; A.F. Sill *et al.*, Phys. Rev. D 48 (1993) 29; R.C. Walker *et al.*, Phys. Rev D 49 (1994) 5671; L. Andivahis *et al.*, Phys. Rev. D 50 (1994) 5491; M.E. Christy *et al.*, Phys. Rev. C 70 (1994) 015206

[25] O. Gayou *et al.*, Phys. Rev. Lett. 88 (2002) 092301.

[26] B.D. Milbrath *et al.*, Phys. Rev. Lett. 80 (1998) 452; *ibid.* 82 (1999) 2221 (E).

[27] J. Arrington, Phys. Rev. C 68 (2003) 034325; *ibid.* C 69 (2004) 022201.

[28] P. Guichon, M. Vanderhaeghen, Phys. Rev. Lett. 91 (2003) 142303; P.G. Blunden, W. Melnitchouk, J.A. Tjon, Phys. Rev. Lett. 91 (2003) 142304; J. Arrington, Phys. Rev. C 69 (2004) 022201; *ibid.* Phys. Rev. C 69 (2004) 032201; Y.C. Chen *et al.*, hep-ph/0403058 (2004).

[29] E.J. Brash, A. Kozlov, Sh. Li, G.M. Huber, Phys. Rev. C 65 (2002) 051001.

[30] P. Mergell, Ulf-G. Meissner, D. Dreschel, Nucl. Phys. A 596 (1996) 367, and references therein; H.-W. Hammer and Ulf-G. Meissner, hep-ph/0312081 (2004).

Figure Captions

Figure 1. Dual-QCD_∞'s form factor $F_1(Q^2)$, Eq.(5.5), for the fitted parameter $\beta_1 = 3.03$, together with the experimental data as corrected in [29].

Figure 2. Dual-QCD_∞'s form factor $F_2(Q^2)$, Eq.(5.5), for the fitted parameter $\beta_2 = 4.20$, together with the experimental data as corrected in [29].

Figure 3. Dual-QCD_∞'s form factor $G_M(Q^2)$, Eq.(2.35), for the fitted parameters $\beta_1 = 3.03$ and $\beta_2 = 4.20$, together with the experimental data as corrected in [29].

Figure 4. Dual-QCD_∞'s ratio $\frac{\mu_p G_E(Q^2)}{G_M(Q^2)}$ for the fitted parameters $\beta_1 = 3.00$ and $\beta_2 = 4.20$, together with the experimental data [8, 24].

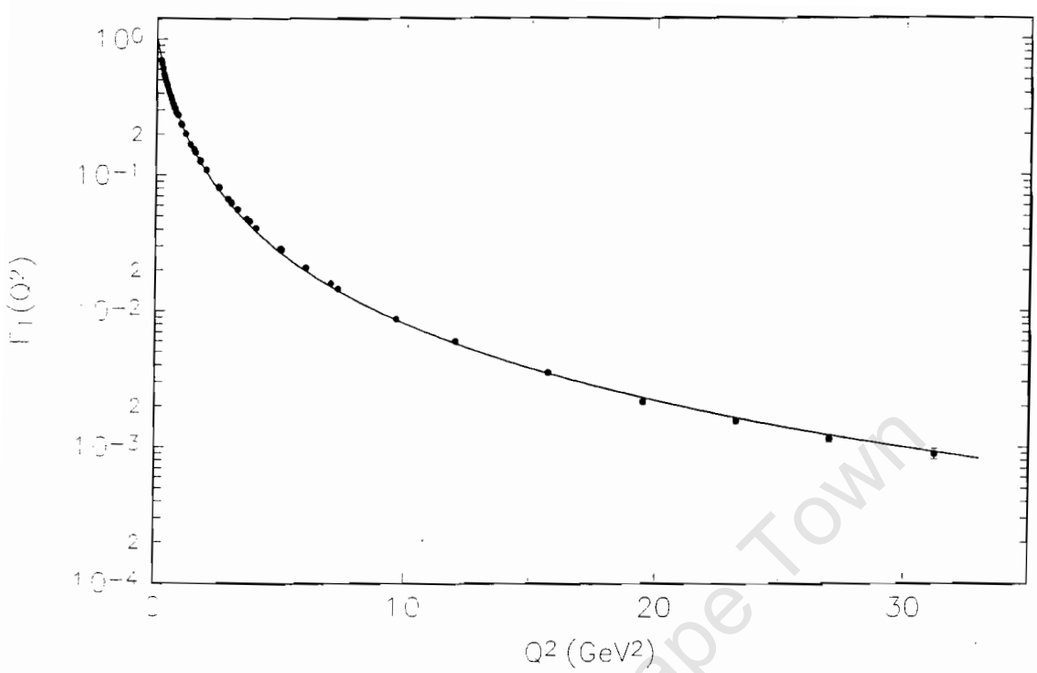

Figure 1:

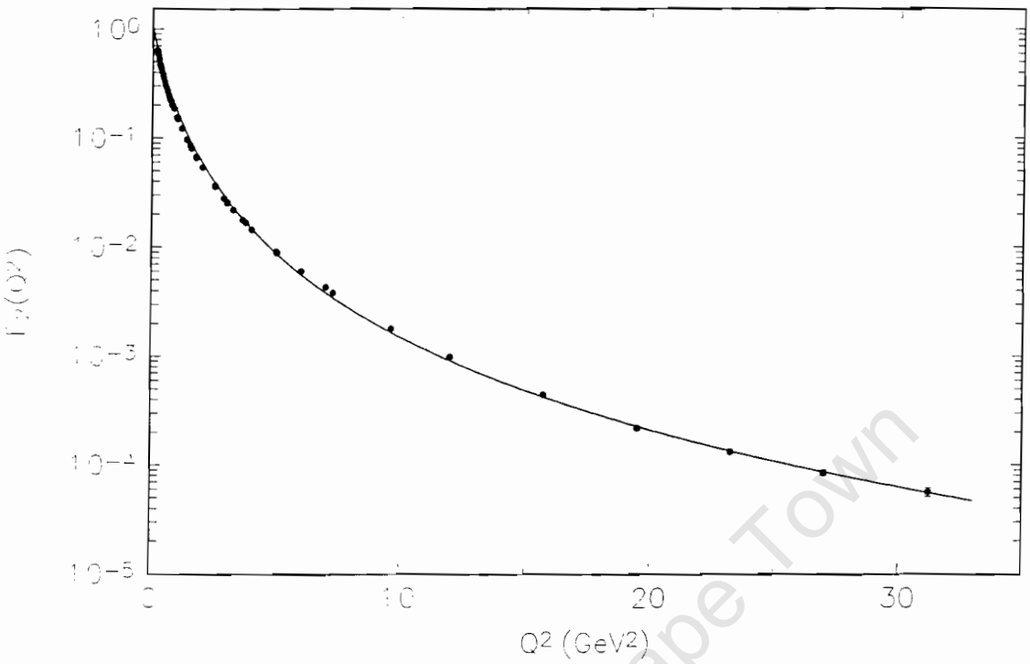

Figure 2:

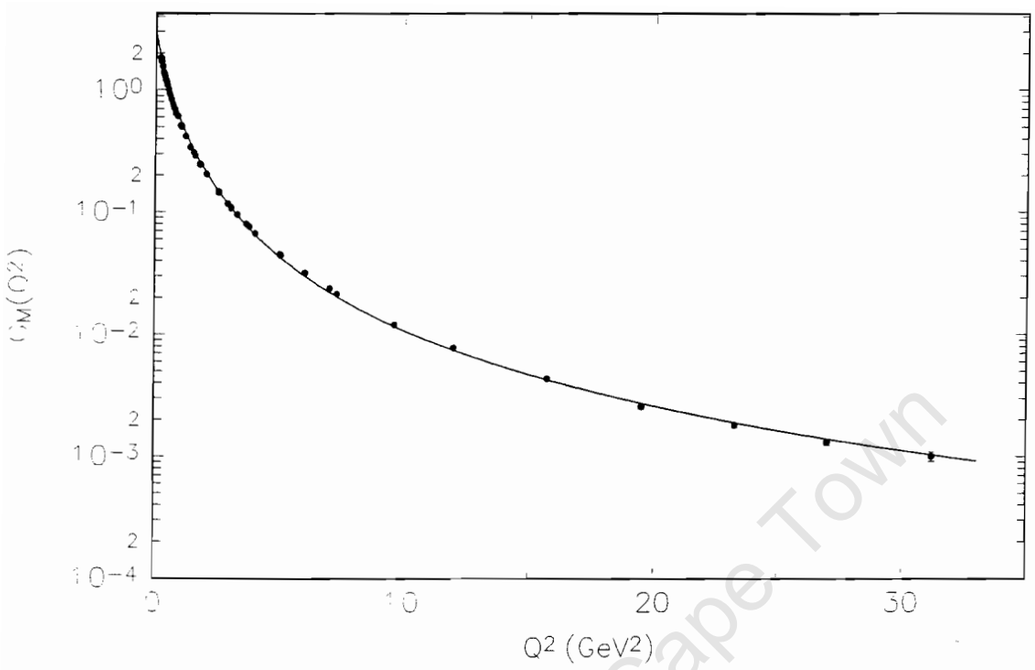

Figure 3:

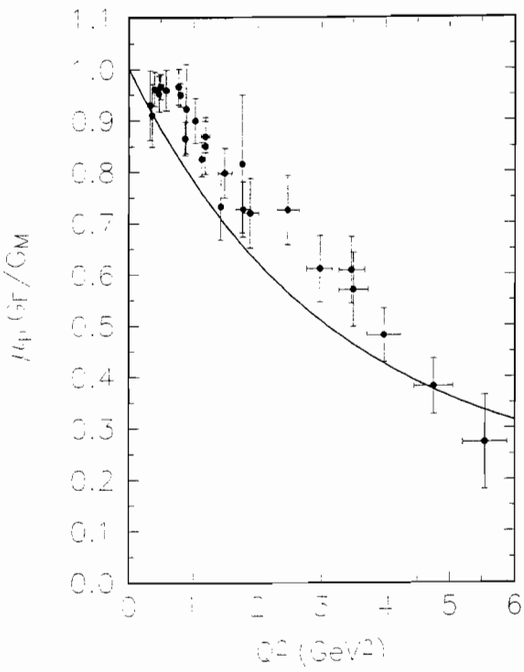

Figure 4: